Impact of half-wave plate systematics on the measurement of cosmic birefringence from CMB polarization

Marta Monelli

Max Planck Institut für Astrophysik
Garching (Germany)

March 28th, 2023

CMB anisotropies

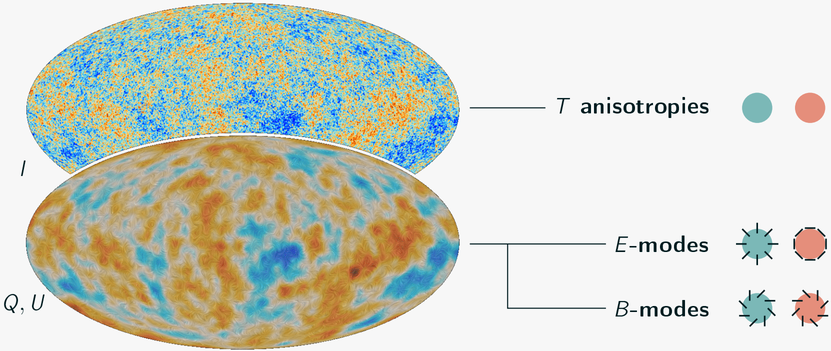

image credit: Jonathan Aumont

searching B-modes from inflation

Expectation: inflation-sourced perturbations leave traces on the CMB polarization.

Large scale B-modes can probe inflation.

Unprecedented sensitivity requirements!

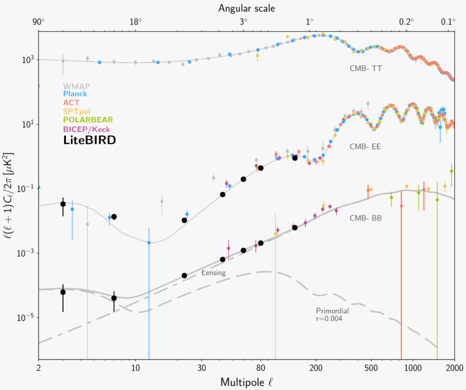

a side effect: measuring cosmic birefringence

CMB might also carry information about
parity-violating new physics: **cosmic birefringence**.
(time-dependent parity-violating pseudoscalar field)

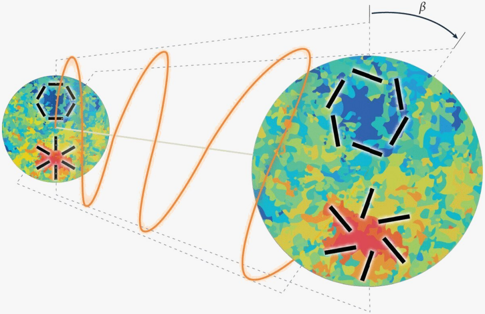

mixing of E and B modes: $$\begin{cases} a^E_{\ell m,\mathrm{obs}} = a^E_{\ell m}\cos 2\beta - a^B_{\ell m}\sin 2\beta, \\ a^B_{\ell m,\mathrm{obs}} = a^E_{\ell m}\sin 2\beta + a^B_{\ell m}\cos 2\beta. \end{cases}$$

image credit: Yuto Minami.

trying to constrain β

$$
\begin{cases}
C_{\ell,\mathrm{obs}}^{TT} = C_\ell^{TT}, \\
C_{\ell,\mathrm{obs}}^{EE} = \cos^2(2\beta)C_\ell^{EE} + \sin^2(2\beta)C_\ell^{BB} - \sin(4\beta)C_\ell^{EB}, \\
C_{\ell,\mathrm{obs}}^{BB} = \cos^2(2\beta)C_\ell^{BB} + \sin^2(2\beta)C_\ell^{EE} + \sin(4\beta)C_\ell^{EB}, \\
C_{\ell,\mathrm{obs}}^{TE} = \cos(2\beta)C_\ell^{TE} - \sin(2\beta)C_\ell^{TB}, \\
C_{\ell,\mathrm{obs}}^{EB} = \sin(4\beta)(C_\ell^{EE} - C_\ell^{BB})/2 + \cos(4\beta)C_\ell^{EB}, \\
C_{\ell,\mathrm{obs}}^{TB} = \sin(2\beta)C_\ell^{TE} + \cos(2\beta)C_\ell^{TB}.
\end{cases}
$$

$$
C_{\ell,\mathrm{obs}}^{EB} = \tan(4\beta)(C_{\ell,\mathrm{obs}}^{EE} - C_{\ell,\mathrm{obs}}^{BB})/2.
$$

trying to constrain β

$$\begin{cases} C_{\ell,\mathrm{obs}}^{TT} = C_\ell^{TT}, \\ C_{\ell,\mathrm{obs}}^{EE} = \cos^2(2\beta)C_\ell^{EE} + \sin^2(2\beta)C_\ell^{BB} - \sin(4\beta)C_\ell^{EB}, \\ C_{\ell,\mathrm{obs}}^{BB} = \cos^2(2\beta)C_\ell^{BB} + \sin^2(2\beta)C_\ell^{EE} + \sin(4\beta)C_\ell^{EB}, \\ C_{\ell,\mathrm{obs}}^{TE} = \cos(2\beta)C_\ell^{TE} - \sin(2\beta)C_\ell^{TB}, \\ C_{\ell,\mathrm{obs}}^{EB} = \sin(4\beta)(C_\ell^{EE} - C_\ell^{BB})/2 + \cos(4\beta)C_\ell^{EB}, \\ C_{\ell,\mathrm{obs}}^{TB} = \sin(2\beta)C_\ell^{TE} + \cos(2\beta)C_\ell^{TB}. \end{cases}$$

$$C_{\ell,\mathrm{obs}}^{EB} = \tan(4\beta)(C_{\ell,\mathrm{obs}}^{EE} - C_{\ell,\mathrm{obs}}^{BB})/2.$$

$$\beta = 0.35 \pm 0.14 \ (68\%\mathrm{CL})$$

Minami and Komatsu (2020) Phys. Rev. Lett. 125

To extract this kind of information from CMB systematics have to be kept under control.

the HWP: reducing systematics

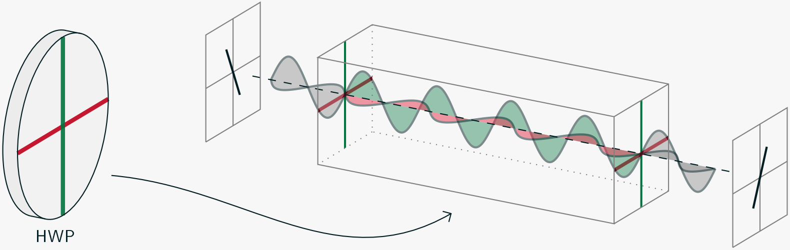

A **rotating** half-wave plate (HWP) as first optical element:

- modulates the signal to $4f_{\mathrm{HWP}}$, allowing to "escape" $1/f$ noise;
- makes possible for a single detector to measure polarization, reducing pair-differencing systematics.

the HWP: inducing systematics

Mueller calculus: radiation described as $S = (I, Q, U, V)$, effect of polarization-altering devices parametrized by $\mathcal{M}$: so that $\mathrm{S}' = \mathcal{M} \cdot \mathrm{S}$.

For an ideal HWP, $\mathcal{M}_{\text{ideal}} = \text{diag}(1, 1, -1, -1)$, but let's look at a realistic case:

$\mathcal{M}_{\text{HWP}} =$

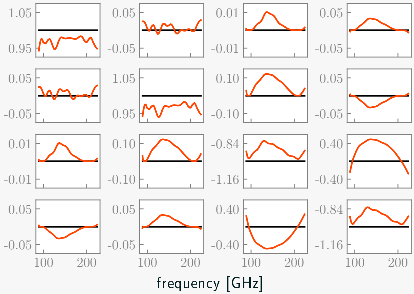

.

how does this affect the observed maps?

steps we took in that direction

- work on a simulation pipeline for a LiteBIRD-like mission;
- simulate observed maps in presence of non-ideal HWP;
- derive analytical formulae to interpret the output.

Monelli et al. (2023) JCAP 03

simulations

what do we simulate

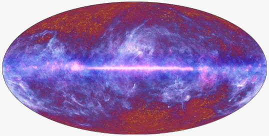

CMB sky maps

image credit: *Planck* collaboration

what do we simulate

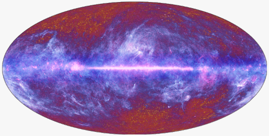

detection

time ordered data (TOD)

map-making

multi-frequency maps

foreground cleaning

CMB sky maps

TOD: collection of the signal detected by *each of the (4508) detectors* during *the whole (3-year) mission*.

image credit: *Planck* collaboration

what do we simulate

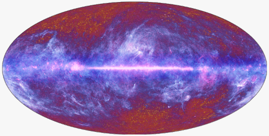

detection

time ordered data (TOD)

map-making

multi-frequency maps

foreground cleaning

CMB sky maps

TOD: collection of the signal detected by *each of the (4508) detectors* during *the whole (3-year) mission*.

Simulating TOD is crucial in the planning of any CMB experiment: helps studying potential systematic effects.

image credit: *Planck* collaboration

sketch of the pipeline

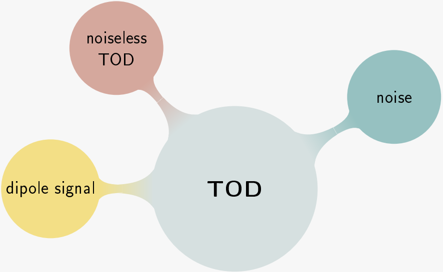

sketch of the pipeline

<u>beamconv</u>: convolution code simulating TOD for CMB experiments with realistic polarized **beams**, scanning strategies and **HWP**.

<u>DUCC</u>: collection of basic programming tools for numerical computation: `fft`, `sht`, `healpix`, `totalconvolve`...

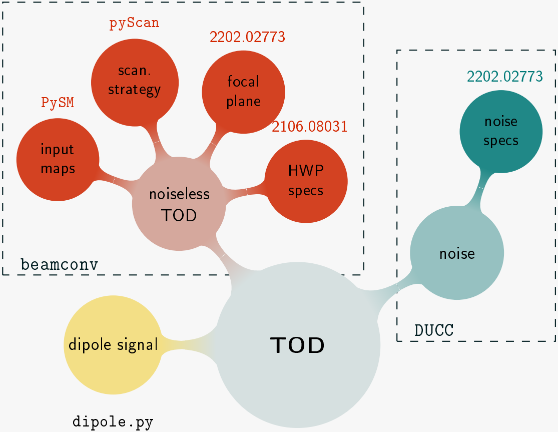

github.com/AdriJD/beamconv, A. Duivenvoorden et al "2012.10437", gitlab.mpcdf.mpg.de/mtr/ducc

working assumptions

To focus on the impact of **HWP non-idealities**, we consider a simplified problem:

- no noise,
- single frequency,
- CMB-only,
- simple beams,
- HWP aligned to the detector line of sight.

input maps

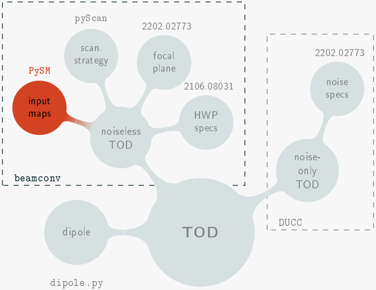

The pipeline can be fed with arbitrary input maps: CMB, foregrounds, or both.

In the paper: I, Q and U input maps with $n_{\mathrm{side}} = 512$ from best-fit 2018 Planck power spectra;

scanning strategy

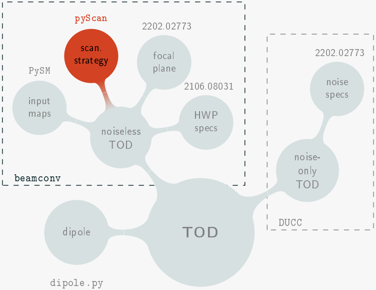

The pipeline can read or calculate pointings. We implemented some functionalities of pyScan in beamconv to deal with satellite missions.

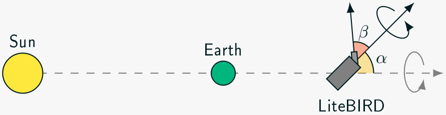

In the paper: 1 year of LiteBIRD-like scanning strategy.

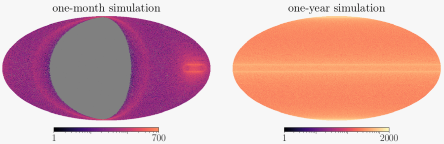

https://github.com/tmatsumu/LB_SYSPL_v4.2

focal plane specifics

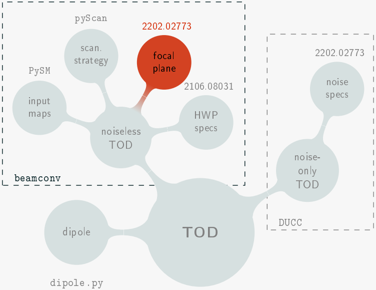

The pipeline can read from the Instrument Model Database (IMO):

```
{'name': 'M02_030_QA_140T',
 'wafer': 'M02',
 'pixel': 30,
 'pixtype': 'MP1',
 [...]
 'pol': 'T',
 'orient': 'Q',
 'quat': [1, 0, 0, 0]}
```

In the paper: 160 dets from M1-140.

specs.	values
f_{samp}	19 Hz
HWP rpm	39
FWHM	30.8 arcmin
offset quats.	[...]

HWP specifics

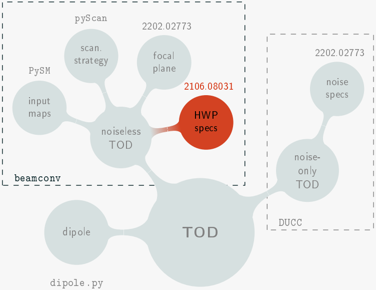

In the paper: HWP is assumed to be ideal in the **first** simulation run (ideal TOD) and realistic in the **second** (non-ideal TOD).

Realistic HWP Mueller matrix elements as shown previously:

$$\mathcal{M}_{\mathrm{HWP}} =$$

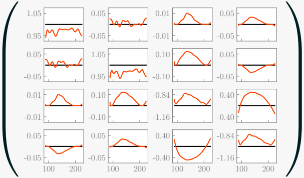

what about maps?

Both ideal and non-ideal TOD processed by **ideal** bin-averaging map-maker.

ideal vs non-ideal output spectra (1)

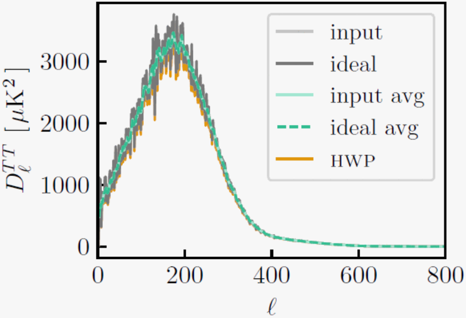

(beam transfer function not deconvolved)

- TT leaked a bit

ideal vs non-ideal output spectra (1)

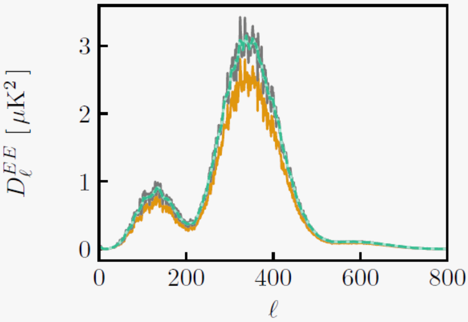

(beam transfer function not deconvolved)

- *TT* leaked a bit
- *EE* leaked a lot!

ideal vs non-ideal output spectra (1)

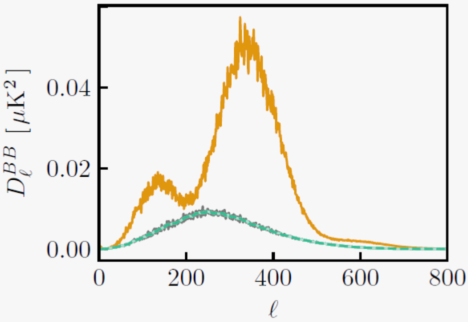

(beam transfer function not deconvolved)

- *TT* leaked a bit
- *EE* leaked a lot!
- *BB* larger (*EE* shape!)

ideal vs non-ideal output spectra (1)

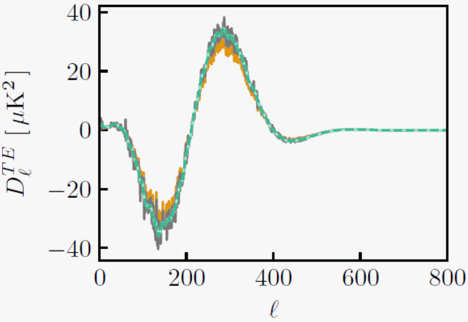

(beam transfer function not deconvolved)

- *TT* leaked a bit
- *EE* leaked a lot!
- *BB* larger (*EE* shape!)
- *TE* leaked a bit

ideal vs non-ideal output spectra (1)

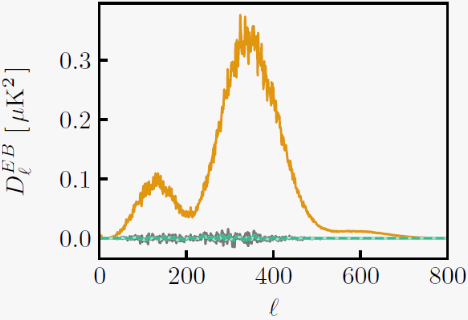

(beam transfer function not deconvolved)

- *TT* leaked a bit
- *EE* leaked a lot!
- *BB* larger (*EE* shape!)
- *TE* leaked a bit
- *EB* non-zero!

ideal vs non-ideal output spectra (1)

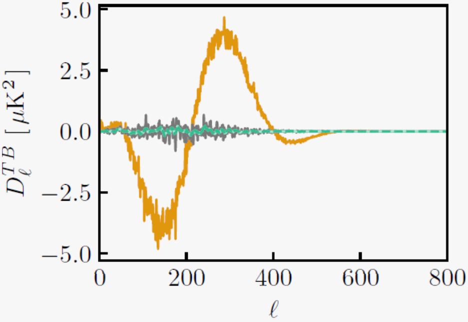

(beam transfer function not deconvolved)

- *TT* leaked a bit
- *EE* leaked a lot!
- *BB* larger (*EE* shape!)
- *TE* leaked a bit
- *EB* non-zero!
- *TB* non-zero!

ideal vs non-ideal output spectra (2)

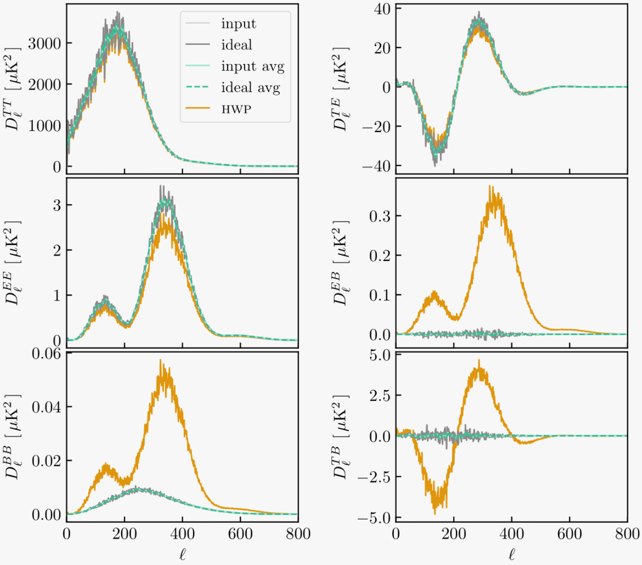

how can we understand this?

modeling the TOD

How `beamconv` computes the TOD:

$$d_t = \sum_{s\ell m} \left[B^I_{\ell s}\, a^I_{\ell m} + \frac{1}{2}\left({}_{-2}B^P_{\ell s}\, {}_2a^P_{\ell m} + {}_2B^P_{\ell s}\, {}_{-2}a^P_{\ell m} \right) + B^V_{\ell s}\, a^V_{\ell m} \right] \sqrt{\frac{4\pi}{2\ell+1}} e^{-is\psi_t}\, {}_sY_{\ell m}(\theta_t, \phi_t)\,,$$

beam coefficients *(or combinations of them if HWP non-ideal)*.

In the paper: $d = (1\ 0\ 0) \cdot \mathcal{M}_{\mathrm{det}} \mathcal{R}_{\xi-\phi} \mathcal{M}_{\mathrm{HWP}} \mathcal{R}_{\phi+\psi} \cdot \mathrm{S}$.

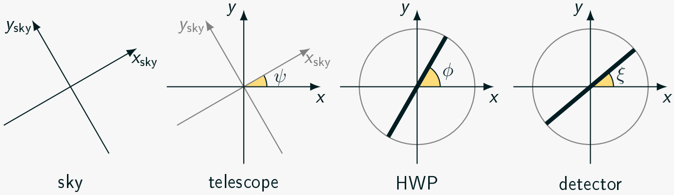

modeling the observed maps

(minimal) TOD: signal detected by 4 detectors.
map-maker: bin-averaging assuming ideal HWP.
estimated output maps: linear combination of $\{I, Q, U\}_{\rm in}$.

$$\begin{pmatrix} d^{(0)} \\ d^{(90)} \\ d^{(45)} \\ d^{(135)} \end{pmatrix} = \begin{pmatrix} (1\ 0\ 0) \cdot \mathcal{M}_{\rm det}\mathcal{R}_{0-\phi}\mathcal{M}_{\rm HWP}\mathcal{R}_{\phi+\psi} \\ (1\ 0\ 0) \cdot \mathcal{M}_{\rm det}\mathcal{R}_{90-\phi}\mathcal{M}_{\rm HWP}\mathcal{R}_{\phi+\psi} \\ (1\ 0\ 0) \cdot \mathcal{M}_{\rm det}\mathcal{R}_{45-\phi}\mathcal{M}_{\rm HWP}\mathcal{R}_{\phi+\psi} \\ (1\ 0\ 0) \cdot \mathcal{M}_{\rm det}\mathcal{R}_{135-\phi}\mathcal{M}_{\rm HWP}\mathcal{R}_{\phi+\psi} \end{pmatrix} \cdot \begin{pmatrix} I_{\rm in} \\ Q_{\rm in} \\ U_{\rm in} \end{pmatrix}$$

Being *ideal*, map-making amounts to apply $(\widehat{A}^T\widehat{A})^{-1}\widehat{A}^T$ to the TOD:

$$\widehat{S} = (\widehat{A}^T\widehat{A})^{-1}\widehat{A}^T A \cdot S.$$

estimated ouput maps

$$
\begin{aligned}
\widehat{I} &= m_{ii} I_{\text{in}} + (m_{iq} Q_{\text{in}} + m_{iu} U_{\text{in}}) \cos(2\alpha) + (m_{iq} U_{\text{in}} - m_{iu} Q_{\text{in}}) \sin(2\alpha)\,, \\
\widehat{Q} &= \frac{1}{2} \Big\{ (m_{qq} - m_{uu}) Q_{\text{in}} + (m_{qu} + m_{uq}) U_{\text{in}} + 2 m_{qi} I_{\text{in}} \cos(2\alpha) + 2 m_{ui} I_{\text{in}} \sin(2\alpha) \\
&\qquad + \big[(m_{qq} + m_{uu}) Q_{\text{in}} + (m_{qu} - m_{uq}) U_{\text{in}} \big] \cos(4\alpha) \\
&\qquad + \big[-(m_{qu} - m_{uq}) Q_{\text{in}} + (m_{qq} + m_{uu}) U_{\text{in}} \big] \sin(4\alpha) \Big\}\,, \\
\widehat{U} &= \frac{1}{2} \Big\{ (m_{qq} - m_{uu}) U_{\text{in}} - (m_{qu} + m_{uq}) Q_{\text{in}} - 2 m_{ui} I_{\text{in}} \cos(2\alpha) + 2 m_{qi} I_{\text{in}} \sin(2\alpha) \\
&\qquad + \big[-(m_{qq} + m_{uu}) U_{\text{in}} + (m_{qu} - m_{uq}) Q_{\text{in}} \big] \cos(4\alpha) \\
&\qquad + \big[(m_{qu} - m_{uq}) U_{\text{in}} + (m_{qq} + m_{uu}) Q_{\text{in}} \big] \sin(4\alpha) \Big\}\,,
\end{aligned}
$$

where $\alpha = \phi + \psi$. For **good** coverage and **rapidly spinning** HWP:

$$
\widehat{\mathsf{S}} \simeq \begin{pmatrix} m_{ii} I_{\text{in}} \\ [(m_{qq} - m_{uu}) Q_{\text{in}} + (m_{qu} + m_{uq}) U_{\text{in}}]/2 \\ [-(m_{qu} + m_{uq}) Q_{\text{in}} + (m_{qq} - m_{uu}) U_{\text{in}}]/2 \end{pmatrix}.
$$

equations for the $\widehat{C}_\ell$s

Expanding $\widehat{S}$ in spherical harmonics:

$$
\begin{aligned}
\widehat{C}_\ell^{TT} &\simeq m_{ii}^2 C_{\ell,\mathrm{in}}^{TT}, \\
\widehat{C}_\ell^{EE} &\simeq \frac{(m_{qq}-m_{uu})^2}{4} C_{\ell,\mathrm{in}}^{EE} + \frac{(m_{qu}+m_{uq})^2}{4} C_{\ell,\mathrm{in}}^{BB} + \frac{(m_{qq}-m_{uu})(m_{qu}+m_{uq})}{2} C_{\ell,\mathrm{in}}^{EB}, \\
\widehat{C}_\ell^{BB} &\simeq \frac{(m_{qq}-m_{uu})^2}{4} C_{\ell,\mathrm{in}}^{BB} + \frac{(m_{qu}+m_{uq})^2}{4} C_{\ell,\mathrm{in}}^{EE} - \frac{(m_{qq}-m_{uu})(m_{qu}+m_{uq})}{2} C_{\ell,\mathrm{in}}^{EB}, \\
\widehat{C}_\ell^{TE} &\simeq \frac{m_{ii}(m_{qq}-m_{uu})}{2} C_{\ell,\mathrm{in}}^{TE} + \frac{m_{ii}(m_{qu}+m_{uq})}{2} C_{\ell,\mathrm{in}}^{TB}, \\
\widehat{C}_\ell^{EB} &\simeq \frac{(m_{qq}-m_{uu})^2-(m_{qu}+m_{uq})^2}{4} C_{\ell,\mathrm{in}}^{EB} - \frac{(m_{qq}-m_{uu})(m_{qu}+m_{uq})}{2} (C_{\ell,\mathrm{in}}^{EE} - C_{\ell,\mathrm{in}}^{BB}), \\
\widehat{C}_\ell^{TB} &\simeq \frac{m_{ii}(m_{qq}-m_{uu})}{2} C_{\ell,\mathrm{in}}^{TB} - \frac{m_{ii}(m_{qu}+m_{uq})}{2} C_{\ell,\mathrm{in}}^{TE}.
\end{aligned}
$$

analytical vs non-ideal output spectra

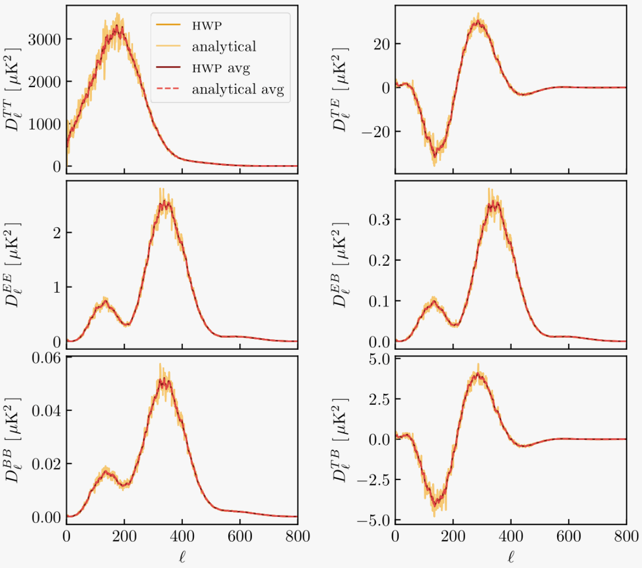

impact on cosmic birefringence

HWP-induced miscalibration

Analytic $\widehat{C}_\ell$s satisfy the relations:

$$\begin{cases} \widehat{C}_\ell^{EB} \simeq \tan(4\widehat{\theta}) \left[\widehat{C}_\ell^{EE} - \widehat{C}_\ell^{BB}\right]/2 \\ \widehat{C}_\ell^{TB} \simeq \tan(2\widehat{\theta})\widehat{C}_\ell^{TE} \end{cases}$$

The HWP induces an additional miscalibration, **degenerate** with cosmic birefringence and polarization angle miscalibration!

HWP-induced miscalibration

Analytic $\widehat{C}_\ell$s satisfy the relations:

$$\begin{cases} \widehat{C}_\ell^{EB} \simeq \tan(4\widehat{\theta}) \left[\widehat{C}_\ell^{EE} - \widehat{C}_\ell^{BB}\right]/2 \\ \widehat{C}_\ell^{TB} \simeq \tan(2\widehat{\theta})\,\widehat{C}_\ell^{TE} \end{cases}$$

our formulae suggest

$$\widehat{\theta} \equiv -\frac{1}{2}\arctan\frac{m_{qu}+m_{uq}}{m_{qq}-m_{uu}} \sim 3.8^\circ,$$

compatibly with simulations.

The HWP induces an additional miscalibration, **degenerate** with cosmic birefringence and polarization angle miscalibration!

This doesn't mean that the HWP will keep us from measuring β, but it shows how important it is to carefully calibrate $\mathcal{M}_{\mathrm{HWP}}$.

simple generalizations

including frequency dependence

How does $d = (1\ 0\ 0) \cdot \mathcal{M}_{\text{det}} \mathcal{R}_{\xi-\phi} \mathcal{M}_{\text{HWP}} \mathcal{R}_{\phi+\psi} \cdot \mathsf{S}$ change when the **frequency dependence** of $\mathcal{M}_{\text{HWP}}$ and signal is taken into account?

$$d = (1\ 0\ 0) \cdot \mathcal{M}_{\text{det}} \mathcal{R}_{\xi-\phi} \int \mathrm{d}\nu \, \mathcal{M}_{\text{HWP}}(\nu) \mathcal{R}_{\phi+\psi} \cdot \mathsf{S}(\nu) \, .$$

Assuming an ideal map-maker and retracing the same steps as before:

$$\widehat{\theta} = -\frac{1}{2} \arctan \frac{\langle m_{qu} + m_{uq} \rangle}{\langle m_{qq} - m_{uu} \rangle}, \qquad \text{where } \langle \cdot \rangle = \int \mathrm{d}\nu \cdot (\nu) S(\nu).$$

instrument miscalibration

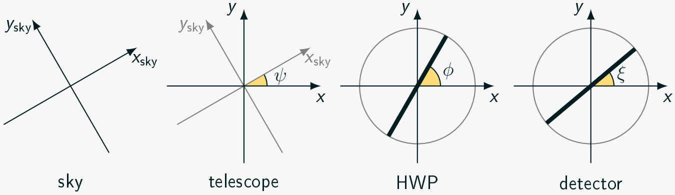

So far, we assumed $\begin{cases} \widehat{\psi} \equiv \psi, \\ \widehat{\phi} \equiv \phi, \\ \widehat{\xi} \equiv \xi, \end{cases}$ but more generally $\begin{cases} \widehat{\psi} \equiv \psi + \delta\phi, \\ \widehat{\phi} \equiv \phi + \delta\psi, \\ \widehat{\xi} \equiv \xi + \delta\xi. \end{cases}$

Taking such (frequency-independent) deviations into account:

$$\widehat{\theta} = -\frac{1}{2}\arctan\frac{\langle m_{qu} + m_{uq}\rangle}{\langle m_{qq} - m_{uu}\rangle} + \delta\theta, \qquad \text{where } \delta\theta \equiv \delta\xi - \delta\psi - 2\delta\phi.$$

steps forward

Even *more general* generalizations worth exploring:

- including a realistic band pass,
- allowing for miscalibrations to depend on ν.

For how long can we push the analytical formulae?

the importance of calibration

how does the map-model change

Without HWP:

$$\begin{pmatrix} I_j \\ Q_j \\ U_j \end{pmatrix} = \sum_\lambda g_\lambda \begin{pmatrix} I_\lambda \\ Q_\lambda \\ U_\lambda \end{pmatrix} + n,$$

With HWP:

$$\begin{pmatrix} I_j \\ Q_j \\ U_j \end{pmatrix} = \sum_\lambda \begin{pmatrix} g_\lambda & 0 & 0 \\ 0 & \rho_\lambda & \eta_\lambda \\ 0 & \eta_\lambda & \rho_\lambda \end{pmatrix} \begin{pmatrix} I_\lambda \\ Q_\lambda \\ U_\lambda \end{pmatrix} + n,$$

where

$$g_\lambda = \frac{\int \mathrm{d}\nu\, G(\nu) m_{ii}(\nu) a_\lambda(\nu)}{\int \mathrm{d}\nu\, G(\nu)},$$

$$\rho_\lambda = \frac{\int \mathrm{d}\nu\, G(\nu)(m_{qq} - m_{uu})(\nu) a_\lambda(\nu)}{\int \mathrm{d}\nu\, G(\nu)},$$

$$\eta_\lambda = \frac{\int \mathrm{d}\nu\, G(\nu)(m_{qu} + m_{uq})(\nu) a_\lambda(\nu)}{\int \mathrm{d}\nu\, G(\nu)}.$$

HWP non-idealities affect gain, polarization-efficiency and cross-pol leakage.

effective SEDs

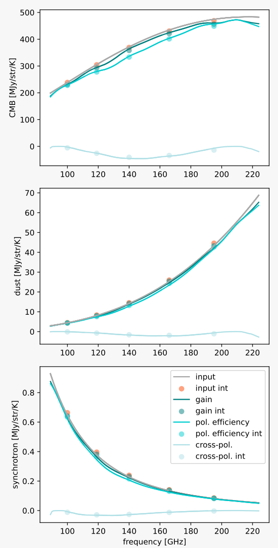

$$\sum_{\lambda} \begin{pmatrix} g_\lambda & 0 & 0 \\ 0 & \rho_\lambda & \eta_\lambda \\ 0 & \eta_\lambda & \rho_\lambda \end{pmatrix} \begin{pmatrix} I_\lambda \\ Q_\lambda \\ U_\lambda \end{pmatrix} + n,$$

- Since all these effects are frequency dependent, they affect each component differently,
- An imprecise calibration of $\mathcal{M}_{\mathrm{HWP}}$ can lead to complications in the component separation step.

- we are now provided with a simulation pipeline that can be easily adapted to study more complex problems (adding noise, more realistic beams...);
- the analytical formulae represent an alternative tool to study the same problems more effectively (but approximately);
- obvious application: exploiting the analytical formulae to derive calibration requirements for the HWP Mueller matrix elements, so that they don't prevent us from detecting B-modes, measuring cosmic birefringence, nor spoil the foreground cleaning procedure.